ATMOSPHERIC NEUTRINO SOURCES: A REVIEW

PAOLO LIPARI
INFN and Dipartimento di Fisica, Università di Roma "La Sapienza"
P. A. Moro 2, 00185 Roma, Italy
E-mail: paolo.lipari@roma1.infn.it

ABSTRACT

This contribution is a review of recent progress in the calculation of the atmospheric neutrino event rates. The effects of systematic uncertainties in this calculation for the interpretation of the data are discussed. The evidence for new physics appears to be very robust. The estimate of the oscillation parameters in the $\nu_\mu \leftrightarrow \nu_\tau$ hypothesis, especially for Δm^2 is limited by systematic uncertainties, but it appears likely that uncertainties connected to the detector response are the dominant effect in the determination of the allowed intervals.

1. Introduction

The comparison of the experimental measurements of the atmospheric ν fluxes performed by Super–Kamiokande (SK)[1,2] and other underground detectors[3,4,5,6] with predictions based on the standard model shows large discrepancies that have been interpreted as evidence for neutrino oscillations or some other form of "new physics". In this contribution we will discuss recent progress in the calculation of the atmospheric ν fluxes, give estimates about the size of the uncertainties in the prediction, and discuss possible consequences in the interpretation of the data.

Before entering into a detailed discussion of the calculation of the atmospheric neutrino fluxes it can be instructive to note that the evidence for oscillations (or other forms of new physics) is qualitatively based on two effects:

- a measured up/down ratio of order ~ 0.5, much smaller than the expected value of unity;
- a measured μ/e ratio $\sim 30\%$, smaller that the expected value $\simeq 2$.

Additional evidence for new physics is obtained from the suppression and the distortion of the zenith angle distribution of ν–induced upgoing muons.

The predictions for the up/down and μ/e ratio can be obtained on the basis of simple elementary considerations and are robust and model–independent. We briefly review these arguments.

Up/Down symmetry. The flux of cosmic rays that reach the surface of the Earth has been thoroughly "isotropized" by the galactic magnetic fields and therefore different points near the Earth's surface receive the same direction–independent flux. This has been verified experimentally to good accuracy. The main correction is due to geomagnetic effects (see the discussion in sec. 2.3). The assumption of isotropy of

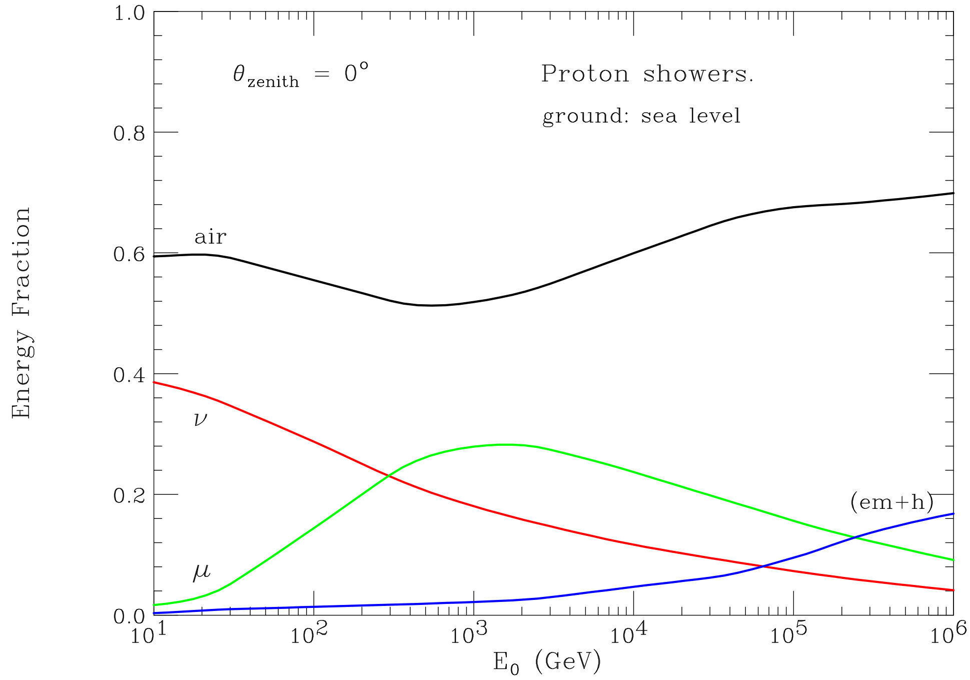

Fig. 1. Fractions of the kinetic energy of a vertical cosmic ray proton transformed into different channels: (i) air ionization, (ii) neutrinos, (iii) muons reaching the ground, (iv) tail of the electromagnetic and hadronic showers that reaches the ground.

the cosmic rays and the spherical shape of the Earth are then sufficient to predict that the ν–fluxes are up–down symmetric, that is:

$$\phi_{\nu_\alpha}(E_\nu, \theta) = \phi_{\nu_\alpha}(E_\nu, \pi - \theta) \tag{1}$$

All ν trajectories (apart the tiny minority that interacts) crosses the Earth surface twice, first down–going and then up–going. The zenith angles at the two crossing points are related by $\theta_{\rm out} = \pi - \theta_{\rm in}$. After integration over the entire Earth's surface there are therefore exactly the same number of atmospheric ν with zenith angle θ and $\pi - \theta$. From spherical symmetry it then follows that the fluxes $\phi_{\nu_\alpha}(E_\nu, \theta)$ and $\phi_{\nu_\alpha}(E_\nu, \pi - \theta)$ must be identical for any flavor and energy.

μ/e ratio. Neutrinos are produced in the decay of pions and kaons, the main source being the chain decay of $\pi^\pm$ such as $\pi^+ \to \mu^+ + \nu_\mu$ followed by $\mu^+ \to e^+ + \nu_e + \overline{\nu}_\mu$. A remarkable fact is that after chain decay the energy of a charged pion energy is shared approximately equally between the four final particles. This is the consequence of the closeness of the pion and muon masses. In fact in the first decay one has $\langle E_\mu \rangle / E_\pi = (1 + m_\mu^2/m_\pi^2)/2 \simeq 0.786 \simeq \frac{3}{4}$. From this one can deduce that for the neutrinos generated by $\pi^\pm$ decay one has

$$\phi_{\nu_\mu}(E_\nu, \Omega_\nu) + \phi_{\overline{\nu}_\mu}(E_\nu, \Omega_\nu) \simeq 2 \left[\phi_{\nu_e}(E_\nu, \Omega_\nu) + \phi_{\overline{\nu}_e}(E_\nu, \Omega_\nu)\right] \tag{2}$$

Note that π^+ and π^- both contribute a pair $(\nu_\mu, \overline{\nu}_\mu)$ but a ν_e or $\overline{\nu}_e$ depending on the charge, therefore:

$$\phi_{\nu_\mu}(E_\nu, \Omega_\nu) \simeq \phi_{\overline{\nu}_\mu}(E_\nu, \Omega_\nu), \tag{3}$$

on the other hand one expects a small excess of ν_e over $\overline{\nu}_e$ reflecting the fact that a larger fraction of the primary proton energy is transfered to π^+ than to π^-.

An approximate estimate of the event rates for atmospheric neutrino can be obtained with elementary considerations. Cosmic rays provide an energy flux of order:

$$\langle E_0 \ \phi_0 \rangle = \int dE \ E \ \phi_0(E) \simeq 1.2 \ \frac{\text{GeV}}{\text{cm}^2 \text{ s sr}} \tag{4}$$

(approximately $\sim$ 70% of this flux is carried by protons, $\sim$ 20% by ionized Helium nuclei, and the remaining $\sim$ 10% by heavier nuclei: CNO, Ne, Mg, Si, Fe). Cosmic rays interact in the Earth atmosphere and generate hadronic showers. Approximately one half to one third of the energy flux of the primary cosmic rays with $E_0 \lesssim 200$ GeV is transformed into a neutrino flux (with the energy shared among ν_μ, $\overline{\nu}_\mu$, ν_e and $\overline{\nu}_e$ with fractions $\sim \frac{1}{3}$, $\frac{1}{3}$, $\frac{1}{6}$ and $\frac{1}{6}$). The remaining energy is mostly dissipated in air as ionization (mostly produced with the absorption of the electromagnetic shower originated by $\pi^\circ \to \gamma\gamma$ decays), a significant fraction goes into muons that reach the ground, with only a small fraction arriving at the surface in the form of an electromagnetic and hadronic shower (see fig. 1). The energy fluxes of neutrinos of different flavors can therefore be estimated as:

$$\langle E_{\nu_\mu} \ \phi_{\nu_\mu} \rangle \simeq \langle E_{\overline{\nu}_\mu} \ \phi_{\overline{\nu}_\mu} \rangle \simeq 2 \ \langle E_{\nu_e} \ \phi_{\nu_e} \rangle \simeq 2 \ \langle E_{\overline{\nu}_e} \ \phi_{\overline{\nu}_e} \rangle \simeq 0.4 \times \frac{1}{3} \ \langle E_0 \ \phi_0 \rangle \simeq 0.15 \ \frac{\text{GeV}}{\text{cm}^2\text{s sr}} \tag{5}$$

The neutrino cross section, to a good approximation, is proportional to the ν energy ($\sigma_\nu(E_\nu) \simeq \sigma_0 \, E_\nu$ with $\sigma_0^\nu \sim 0.67$ and $\sigma_0^{\overline{\nu}} \sim 0.34$ in units 10^{-38} cm^2/GeV). Therefore the neutrino event rates in an underground detector, in first approximation, depend only on the total energy flux in neutrinos and not on the precise shape of their energy spectrum (a harder spectrum results in fewer neutrinos with a larger cross section). One can then estimate:

$$\begin{aligned} R_{\nu_\mu} \simeq 2 \, R_{\nu_e} \ & \simeq \ N_A \int d\Omega \int dE_\nu \ \phi_\nu(E_\nu) \ [\sigma_0^\nu \, E_\nu] \\ & \simeq \ N_A \ [4\pi] \ \sigma_0^\nu \ \langle E_\nu \, \phi_\nu \rangle \simeq 100 \text{ events/(Kton year)} \end{aligned} \tag{6}$$

(where $N_A = 6.023 \times 10^{32}$ nucleons/Kton) in qualitative agreement with the data. It is very difficult to imagine mechanisms in the standard model that would modify this prediction of a strict relation between the fluxes of neutrinos with different flavors, while the experimental data suggests a suppression of order 30–40% of the ν_e and $\overline{\nu}_e$ fluxes relative to the ν_μ and $\overline{\nu}_\mu$ fluxes. This is well outside the systematic uncertainties of the prediction and can only be explained either with the existence of a large experimental error in the flavor determination, or with the existence of new phenomena.

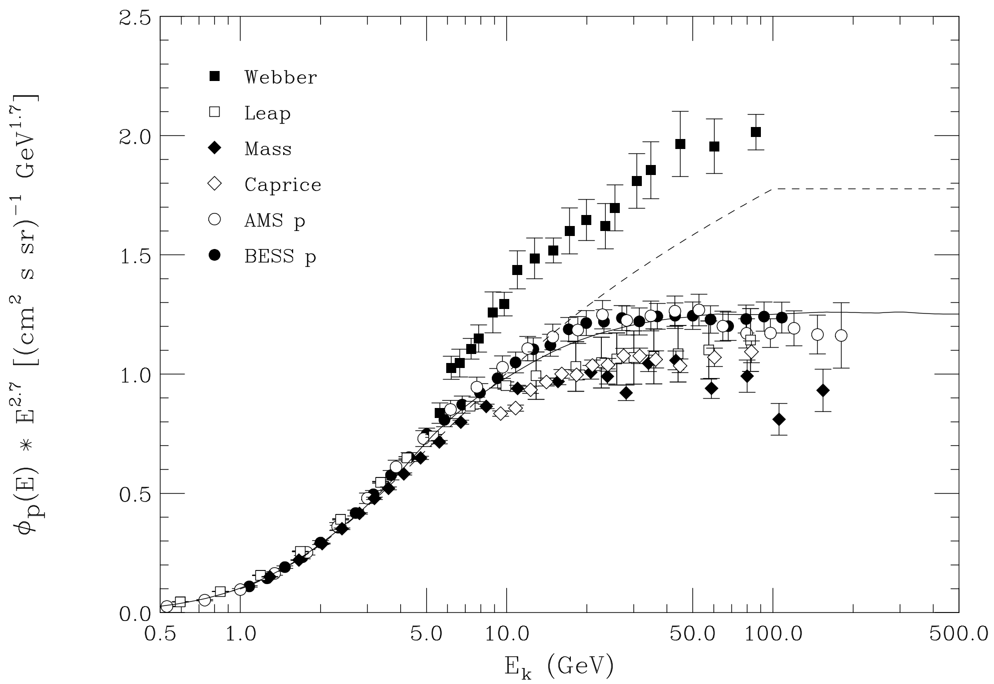

Fig. 2. Measurements of the cosmic ray proton flux with magnetic detectors. The lines are the representations of the flux used by the Bartol[10)] and HKKM[11)] calculations.

A calculation of the atmospheric ν fluxes is based on three fundamental elements: (i) a description of the primary cosmic ray (c.r.) fluxes. (ii) a model for particle production in hadronic interactions and (iii) a calculation scheme to obtain the neutrino fluxes that reach a certain detector.

In the next three sections will discuss these three elements, in section 5 we discuss the constraints of the muon measurements, in section 6 we dicuss the different calculations of the atmospheric neutrino fluxes available in the literature. Section 7 contains a discussion of the effects of systematic uncertainties on the determination of the oscillation parameters in the hypothesis of $\nu_\mu \leftrightarrow \nu_\tau$ oscillations.

2. The primary cosmic ray fluxes

2.1. The proton flux

The fluxes of primary particles reaching the Earth have to be measured with detectors placed at high altitude on balloons or satellites. Several measurements of the proton flux are plotted as a function of energy after multiplication by the factor $E_{\rm kin}^{2.7}$ in fig.2. Our knowledge of the flux has improved dramatically in recent years. The most recent measurements of AMS[16)] and BESS[17)] have relatively small uncertainties and are in very good agreement with each other (to within 5%). The reasons behind the large discrepancies with earlier results, especially the higher normalization points of Webber et al[18], but also the lower normalization results of Caprice[19] are not understood, but are likely to be the consequence of systematic errors. It appears reasonable to consider the proton flux as well determined up to a maximum energy of $E_0 \sim 100$–200 GeV.

The measurements of the proton flux performed with magnetic spectrometer stop at a rigidity $p/Z \sim 100$ GV, due to the detector resolution and limited exposure. The calculation of the rates of sub–GeV and multi–GeV events in a ν detector requires only a modest extrapolation. However for the calculation of up-going muon events, produced by higher energy neutrinos, one needs an extrapolation up to $E_0 \sim 10^5$ GeV. The extrapolation to higher energy and an estimate of the systematic uncertainty of this extrapolation are a non trivial problem. Direct measurements up to an energy $E_p \lesssim 3 \times 10^5$ GeV, have been performed with emulsion chambers on balloon as for example by JACEE[21]. In fig. 3 we show an example of an extrapolation together with the JACEE data, and the old set of data of RYAN[20] renormalized with a multiplicative factor of 0.75 that is equivalent to a recalibration of the detector.

2.2. Helium and heavier nuclei contributions

Both the AMS[23]and BESS[17] experiments have also measured the Helium flux. In this case the results show a 10% discrepancy when plotted as a function of rigidity. In fig. 3 we show the data points of the experiments together with the result of JACEE[21] and an example of a fit. The Helium component accounts for approximately ~ 20 % of the atmospheric neutrino event rate. There is some indication that the Helium c.r. flux is a little flatter than the proton one, a result of significant interest for cosmic ray physics. In the near future the BESS experiment is planning a new exposure with an improved detector, while the AMS detector is planning a long term exposure on the International Space Station. These measurements should allow to extend the direct measurement of the p and He flux of one order of magnitude, determining unambiguosly if the indication of different slopes is real, and reducing significantly the uncertainties due to the high energy extrapolation.

Measurements of the most abundant components of cosmic rays with $Z \geq 3$ obtained by the HEAO–3[31] and CRN detectors (both on satellites) are shown in fig. 4, together with fits to the individual components. Cosmic rays with $(Z \geq 3)$ account for $\sim 10\%$ of the ν event rate, therefore uncertainties of the intensity of the heavy component is not too important in the determination of the neutrino rate. This is not in contrast with the result that cosmic rays become an important component of the cosmic ray fluxes at high energy *per particle*. For a cosmic ray particle of mass number A and total energy $E_{\rm tot}$ one can make the approximation that it is equivalent to a set of A nucleons with an energy per nucleon $E_0 = E_{\rm tot}/A$. The set of fluxes

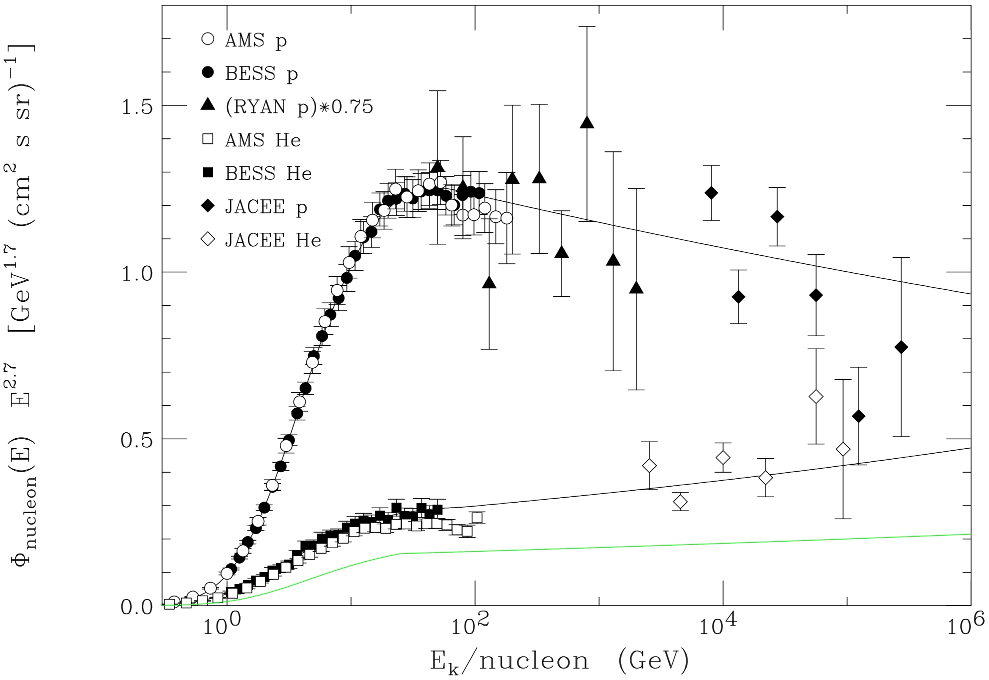

Fig. 3. Measurements of the cosmic ray proton and Helium fluxes. including higher energy measurements.

$\phi_A(E_{\rm tot})$ of nuclei with mass A and total energy $E_{\rm tot}$ correspond to a nucleon flux:

$$\phi_{\rm nucleon}(E_0) = \sum_A A \, \frac{dE_{\rm tot}}{dE_0} \, \phi_A(E_0 \, A) = \sum_A A^2 \, \phi_A(E_0 \, A) \tag{7}$$

A particle flux with power law form $\phi_A(E_{\rm tot}) \simeq K_A \, E_{\rm tot}^{-\alpha}$ correspond to a nucleon flux $\phi_{\rm nucleon}(E_0) \simeq (K_A \, A^{-\alpha+2}) \, E_0^{-\alpha}$. For $\alpha > 2$, as is the case in nature, the importance of the heavy component is suppressed relatively to the light one by a factor $A^{-\alpha+2} \simeq A^{-0.7}$. In fig. 5 we show the contributions of the proton, helium, and $Z \geq 3$ components to the particle fluxes plotted as a function of energy per particle. A subset of experimental results from Extensive Air Shower detectors is also shown. A critical discussion of these results is beyond the scope of this review. Note that in fig. 3 and 5 the scale of the x (energy) axis is logarithmic and extends for several decades while the scale of the y axis (flux multiplied by $E^{2.7}$) is *linear* in the figure. This allow to show clearly how closely the high energy cosmic ray fluxes follow for several decades a power law behaviour, with an exponent not far from $\alpha \simeq 2.7$ for all components. An estimate of an uncertainty on the slope $\delta\alpha \simeq 0.05$, appears as reasonable.

2.3. Geomagnetic effects

In order to compute the atmospheric neutrino fluxes one needs to know the flux

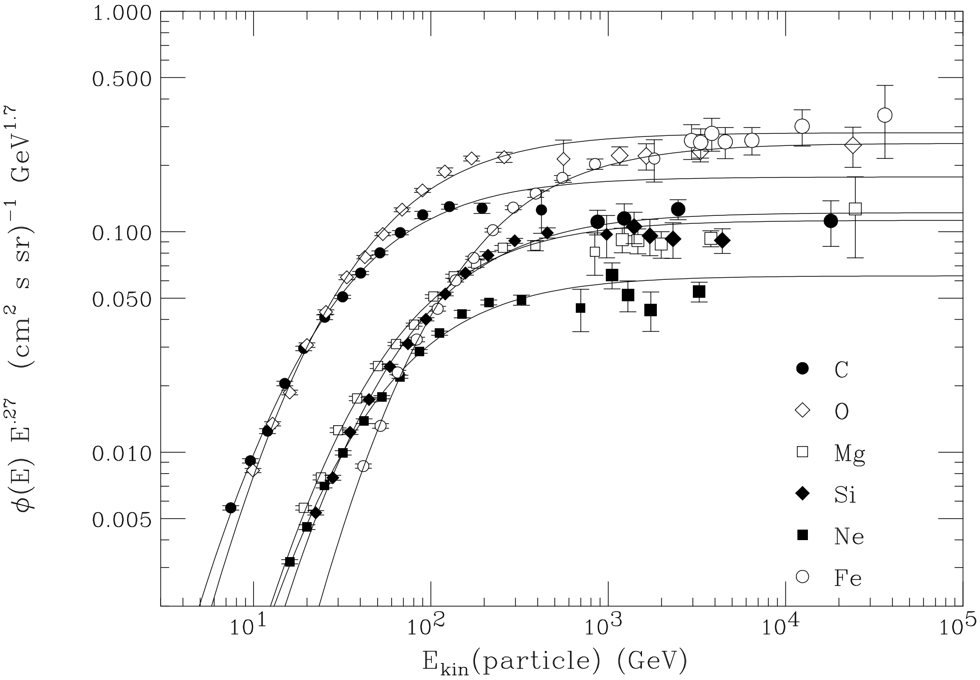

Fig. 4. Measurements of the fluxes of heavy nuclei by the HEAO–3[31)] (small points) and CRN[32)] (large points) experiments.

of cosmic rays that reach all points on the surface of the Earth. It has been known for several decades that the geomagnetic field has an important influence on the cosmic rays fluxes, and that the fluxes reaching the regions close to the geomagnetic poles is much stronger than the flux reaching the Earth's magnetic equatorial region. An accurate description of these geomagnetic effects is clearly needed.

In the calculation of the atmospheric neutrinos the flux of cosmic rays reaching a point $\vec{x}$ with momentum $\vec{p}$ has been modeled as:

$$\phi(\vec{x},\vec{p}) = \phi_\infty(p) \times \begin{cases} 1 & \text{for "allowed" trajectories,} \\ 0 & \text{for "forbidden" trajectories.} \end{cases} \tag{8}$$

where $\phi_\infty(p)$ is an isotropic flux present at large distances from the Earth. The trajectory, defined by the values ($\vec{x}$,$\vec{p}$) and the particle electric charge, is considered "allowed" or "forbidden", according to the results of a numerical study of its past history performed integrating the classical equation of motion in a magnetic field. Trajectories that originate at large distances from the Earth are allowed, all other ones are forbidden. Equation (8) can be deduced as a simple consequence of the Liouville theorem under two assumptions:

(i) the cosmic ray flux at large distances from the Earth is isotropic and time and position independent, and given by $\phi_\infty(p)$;

(ii) the motion of cosmic rays can be simply described as classical trajectories in a static magnetic field.

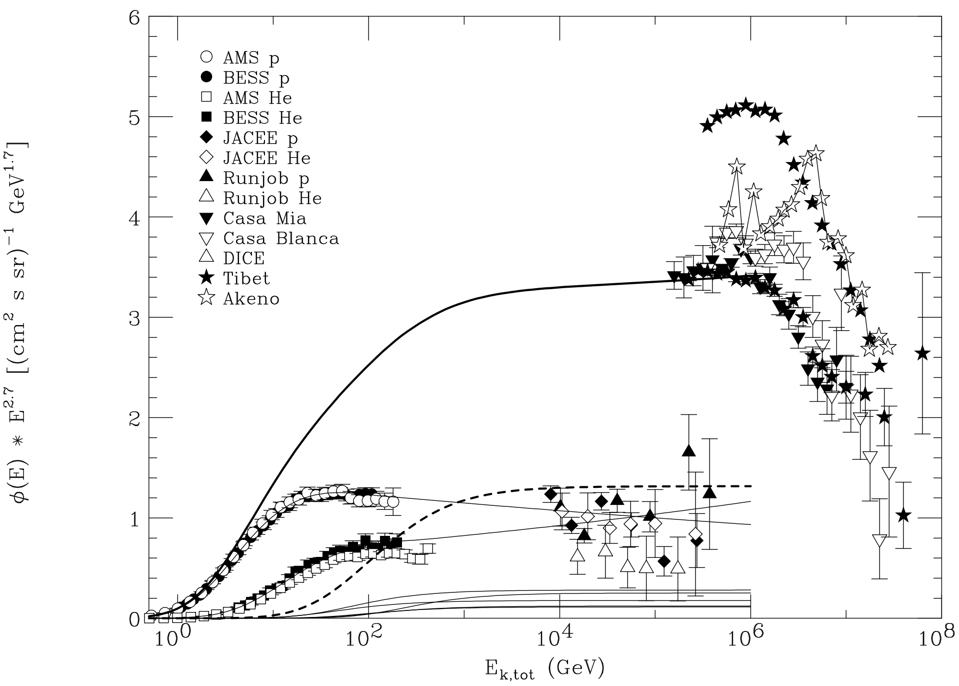

Fig. 5. Contributions of the p helium, and $Z \geq 3$ components to the particle fluxes plotted as a function of energy per particle. A subset of experimental results from Extensive Air Shower detectors is also shown.

The flux of particles with momentum $\vec{p}$ at the point $\vec{x}$ and time t is related to the phase space density by:

$$\phi(\vec{x},\vec{p},t) = \beta\,|\vec{p}|^2\ \frac{d^6N}{d^3p\,d^3x}(\vec{x},\vec{p},t) = \beta\,|\vec{p}|^2\ n(\vec{x},\vec{p},t) \tag{9}$$

where β is the particle velocity and we used the notation $n = d^6N/(d^3pd^3x)$. If a particle at the time t_i is at large distances from the Earth in the position $\vec{x}_i$ with momentum $\vec{p}_i$, it is easy to see that at any later time t when the particle is at the position $\vec{x}$ with monentum $\vec{p}$ one has:

$$n(\vec{x},\vec{p},t) = n(\vec{x}_i,\vec{p}_i,t_i) = n_\infty(p_i) = n_\infty(p). \tag{10}$$

In the first equality we have used the Liouville theorem that states that the phase space density is a constant of motion, in the second one the assumption of an isotropic, homogeneous and time independent flux at large distances from the Earth, and in the third one the fact that for motion in a static magnetic field the absolute value of the momentum is constant ($p_i = p$). Equation (10) gives the first line of the algorithm (8): the flux $\phi(\vec{x},\vec{p})$ at an arbitrary point $\vec{x}$ for arbitrary momentum $\vec{p}$ is equal to the asymptotic isotropic flux $\phi_\infty(p)$ if the phase space point $(\vec{x},\vec{p})$ is connected by a particle trajectory to a phase space point "at infinity", that is for all allowed trajectories. The argument we have outlined does not tell us anything about

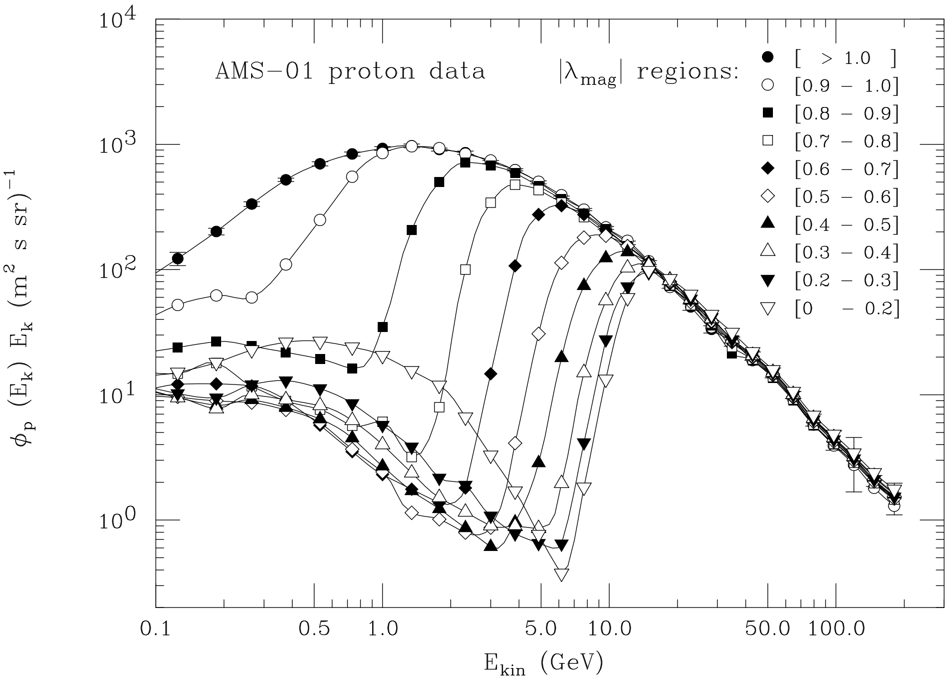

Fig. 6. Cosmic ray proton flux measurements of the AMS detector [16] averaged for a detector position in ten regions of magnetic latitude. The error bars are shown only for one set of measures ($|\lambda_{mag}| > 1$ radiant).

the flux coming from forbidden trajectories, however it is intuitive that the flux must be small because, by definition, no particles can arrive along these trajectories from the large reservoir of particles at large distances, and only particle produced locally can contribute to the flux from these trajectories. As it will be discussed below, the interaction of cosmic rays in the atmosphere does generate a small "albedo" flux of secondary particles that populates the forbidden trajectories. This albedo flux has however a negligible effect on the production of neutrinos.

Important confirmations about the validity of the algorithm (8) to describe the geomagnetic effects on the cosmic rays fluxes have been obtained with the data of a ten days flight of the Anti Matter Spectrometer (AMS) aboard the Space Shuttle in June 1998. The AMS detector has measured the cosmic ray flux at an altitude of ~ 400 Km over a large fraction of the Earth surface. The results for the proton flux[16] are shown in fig. 6, where the flux of vertical protons is plotted as a function of the kinetic energy. The 10 different sets of points correspond to the measurements taken when the detector was in different regions of magnetic latitude. One can immediately note several points.

(i) The fluxes measured in different geographycal regions are equal (within errors) for kinetic energy $E_k \gtrsim 15$ GeV, in agreement with (8). This is perhaps the best evidence for the isotropy of cosmic rays for very large angular scales (additional evidence for isotropy has been obtained with detectors located at a fixed point, using the rotation

of the Earth to change the observation cone).
(ii) A magnetic "cutoff" at a momentum that is largest when the detector is near the geomagnetic equator.[a] The form of the geomagnetic cutoff is in good quantitative agreement with the results of the back tracing algorithms that has been used in the past (see[24]) for a discussion).
(iii) It is also evident the presence of non vanishing fluxes of sub–cutoff particles. The measurement of several striking properties of the fluxes of sub–cutoff particles (p, He, $e^\pm$) by AMS[16,23,22]) have generated interest, and lead to speculations that something is missing in our understanding of cosmic rays near the Earth. Examples of the interesting properties of the sub–cutoff particles are a ^{3}He/^{4}He ratio of order ~ 10, an e^+/e^- ratio of order ~ 4, the fact that calculating the past and future trajectories of the sub–cutoff particles detected at the altitude of ~ 400 Km, it appears that they are created and absorbed in well defined regions of the Earth surface that are distinct for positively and negatively charged particles, (with the source region of positively charged particles being the sink of the negatively charged ones and viceversa). The simplest and most natural hypothesis, that the sub–cutoff particles are generated as secondary products of primary cosmic ray interactions in the atmosphere can reproduce well the measurements, and the set of "striking" properties of the sub–cutoff fluxes can have simple and transparent explanations (see[24]) for a discussion).

A conservative estimate of the rate of neutrino events due to subcutoff protons is of order 10^{-2} events/(kton year). These events have a non trivial angular distribution because of the peculiar effects of the geomanetic trapping, however the rate is neglibly small when compared with the observed rate (~ 100 in the same units). To calculate this estimate one can convolute the measured sub–cutoff fluxes at the Space Shuttle orbit with an "event yield" for ν charged current interactions. For example, for μ events the yield is defined as:

$$Y_\mu(E_p) = N_A \int dE_\nu \left[\frac{dn_{p\to\nu_\mu}}{dE_\nu}(E_\nu, E_p)\ \sigma_{\nu_\mu}(E_\nu) + \frac{dn_{p\to\overline{\nu}_\mu}}{dE_\nu}(E_\nu, E_p)\ \sigma_{\overline{\nu}_\mu}(E_\nu)\right] \quad (11)$$

where $dn_{p\to\nu_\mu}/dE_\nu$ and $dn_{p\to\overline{\nu}_\mu}/dE_\nu$ are the average number of ν_μ and $\overline{\nu}_\mu$ with energy E_ν produced in the shower of a proton of energy E_p, σ_{ν_μ} and $\sigma_{\overline{\nu}_\mu}$ are the cross sections for ν_μ and $\overline{\nu}_\mu$ charged current interactions[35]) and N_A is Avogadro's number. The convolution of the ν event yield with the AMS proton–flux measured at high and low magnetic latitudes is shown in fig. 7. The integral of this convolution is ~ 8.4 (kton yr sr)$^{-1}$ for the high magnetic latitude region and ~ 5.7 (kton yr sr)$^{-1}$ for the magnetic equatorial region. The difference between the two rates represents the maximum possible size of geomagnetic effects. In the equatorial region the contribution due to subcutoff protons, obtained integrating for $E_k < 6$ GeV, is

[a] The "cutoff" appears as smooth, because the measurements of the flux are averaged over a large area and a finite angle (a cone of approximately 30°). For a fixed position and a fixed direction the cutoff is predicted to be much sharper, and can be reasonably well approximated as step function.

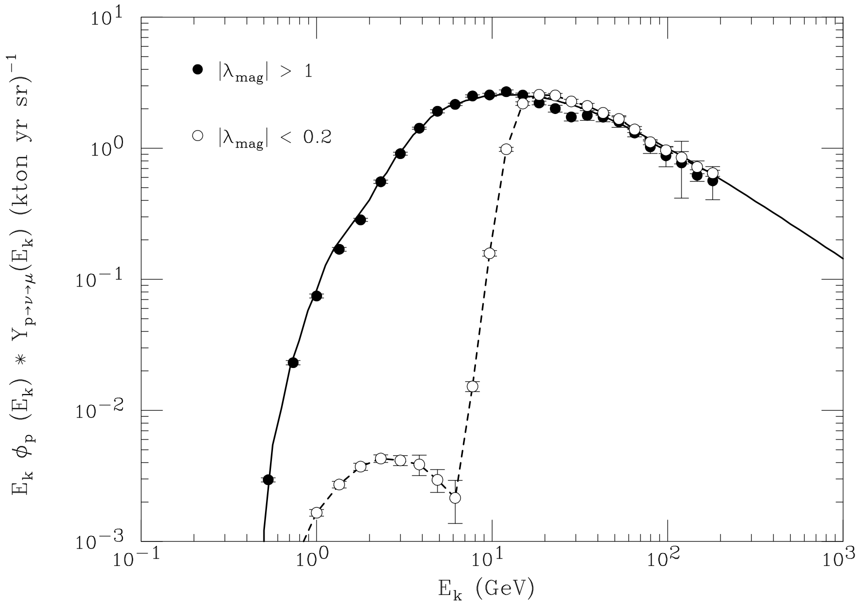

Fig. 7. Convolution of the neutrino event yield for vertical protons with the fluxes observed at high altitude by the AMS detector in two regions of geomagnetic latitude.

$\simeq 0.009$ (kton yr sr)$^{-1}$, that is 0.16% of the total. The smallness of the contribution of the sub–cutoff particles to the ν rate, is a consequence of their softness. In the region considered, at the altitude of the Space Shuttle orbit, the sub–cutoff protons represent $\sim 42\%$ of the particle flux, but only $\sim 1.8\%$ of the energy flux, moreover only 60% of the subcutoff protons is above the kinematical threshold for ν production, and the ν that are produced are soft with low cross section. The integration over solid angle of the effect is non trivial, however we can observe (see fig. 6) that the albedo spectrum has maximum intensity in the magnetic equatorial region, therefore simply multiplying by 4π we are making a conservative overestimate. An additional correction[24)] of order 0.05–0.1 must be included to take into account that the albedo flux at high altitude is enhanced because of the magnetic trapping. In summary the contribution of sub–cutoff particles to the ν fluxes is negliby small.

3. Hadronic Interactions

The modeling of hadronic interactions is obviously important for the estimate of the atmospheric ν fluxes. To illustrate this point let us consider the interactions of a projectile proton with an "air" nucleus at rest. In fig. 9 we plot as a function of the kinetic energy $E_{\rm kin}$ of the projectile the average energy fraction carried away by pions (f_π), kaons (f_K) and nucleons (f_N, in this last case we only consider the kinetic energy of the particles):

$$f_\pi \;=\; \frac{1}{E_{\rm kin}} \sum_{j\in\{\pi^+,\pi^-,\pi^\circ\}} E_j$$

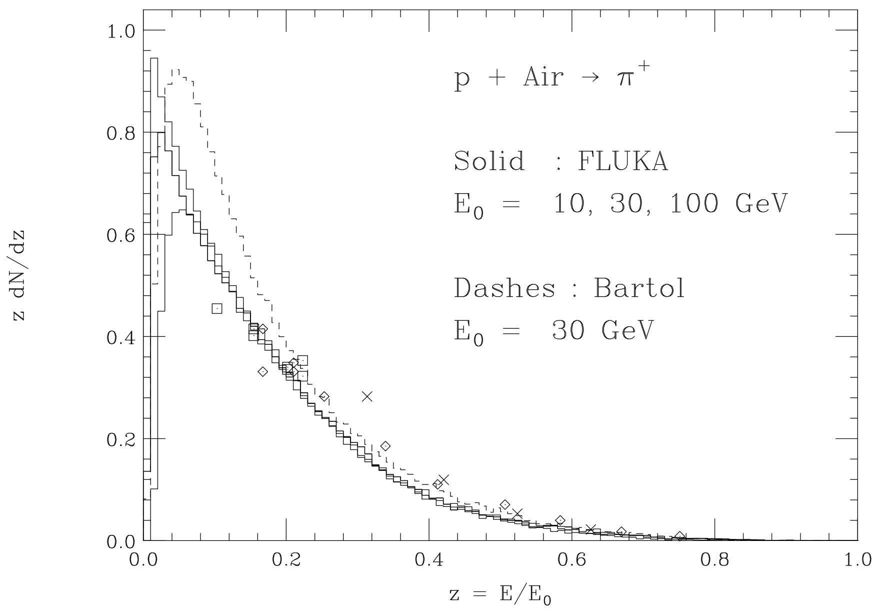

Fig. 8. Inclusive differential cross section for π^+ production for the Bartol and Fluka models.

$$f_K = \frac{1}{E_{\rm kin}} \sum_{j\in\{K^+,K^-,K_L\}} E_j$$

$$f_N = \frac{1}{E_{\rm kin}} \sum_{j\in\{p,n\}} (E_j - M_j)$$

Since all other channels are negligible one has $f_\pi + f_K + f_N \simeq 1$. The solid and dashed curves in fig. 9 are for the hadronic interaction models of FLUKA[12)] and TARGET (the model used in the Bartol calculation[10)]). In fig. 10 we plot the energy fractions f_{π^+}, f_{π^-} and f_{π° that go into pions of different charge. Several features are apparent from the figures. The energy fractions are approximately constant for $E_{\rm kin} \gtrsim 1$ GeV, reflecting the approximate validity of Feynman scaling in the model. At low energy f_π decreases, this is a reflection of the fact that an approximately constant amount of energy $\Delta E_{\rm frag}$ is absorbed in the fragmentation of the target nucleus, and with decreasing projectile energy this represents a larger and larger contribution to f_N. Uncertainties in the properties of the interactions are reflected in differences between the models. For example for $E_{\rm kin} \lesssim 100$ GeV the FLUKA model transfers less energy into pions, with the difference being most important at low $E_{\rm kin}$. In fig. 10 one can also see that in TARGET the energy fractions transfered to pions of different charges have the ordering $f_{\pi^+} > f_{\pi^\circ} > f_{\pi^-}$, while in FLUKA $f_{\pi^+} \simeq f_{\pi^\circ} > f_{\pi^-}$.[b] The large energy transfered into π° in FLUKA is the effect of the production of resonances (including η and η') and their decay branching ratios. Note also the ratio f_{π^+}/f_{π^-} is larger in FLUKA than in TARGET.

[b]In the FLUKA calculation, for $E_{\rm kin}$ between approximately 4 and 200 GeV one has $f_{\pi^0} > f_{\pi^+}$.

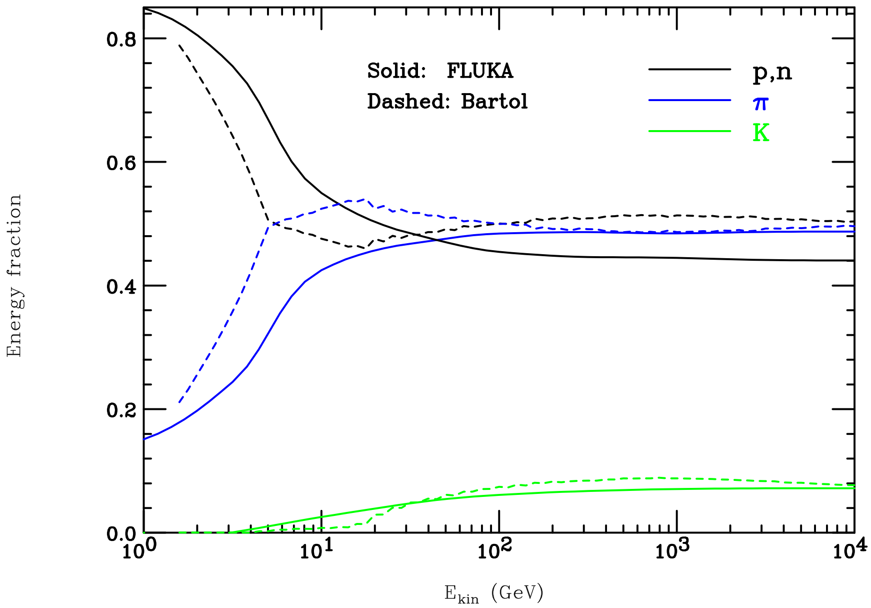

Fig. 9. Fraction of the kinetic energy of a projectile p that goes into nucleons, pions and kaons, plotted as a function of $E_{\rm kin}$. The curves are calculated with the TARGET[10] and FLUKA[12] interaction models.

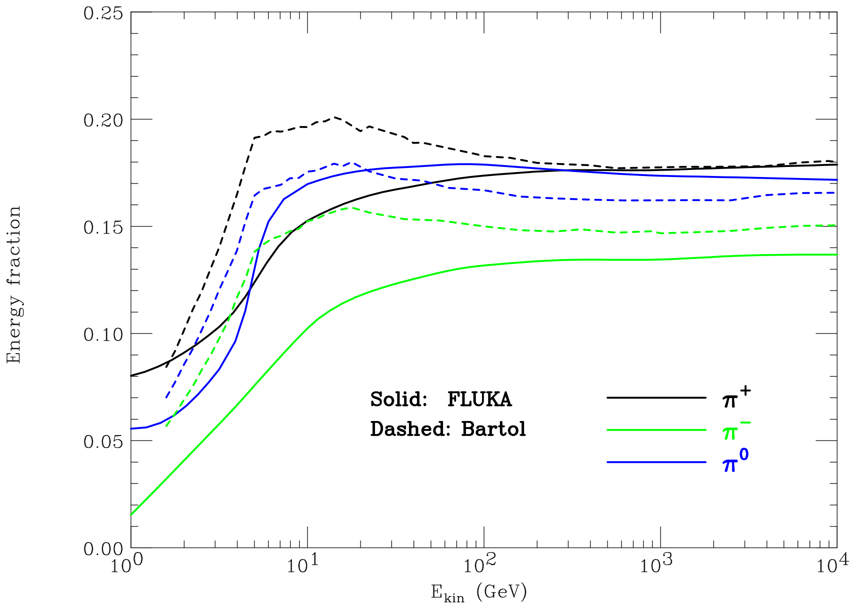

Fig. 10. Fraction of the kinetic energy of a projectile p that goes into π^+, π^- and π°.

In the final state of one interaction one finds the fragments of the target nucleus, a leading nucleon that carries the baryon number of the projectile, a number of mesons, mostly pions, with a non negligible contribution of kaons. In addition one has to consider the production of nucleon–antinucleon pairs and of heavy flavors, these effects are however of small importance at the energies that are relevant for atmospheric neutrinos. Most neutrinos are produced in the chain decay of the charged pions such as $\pi^+ \to \mu^+\nu_\mu$ followed by $\mu^+ \to e^+\nu_e\overline{\nu}_\mu$, with $K^\pm$ and K_L giving smaller contributions. The decay lenghths of pions, kaons and muons (in units of meters) are: $\ell_{\pi^\pm} = 55.9\ p_{\rm GeV}$, $\ell_{K_L} = 31.2\ p_{\rm GeV}$, $\ell_{K^\pm} = 7.5\ p_{\rm GeV}$, and $\ell_{\mu^\pm} = 6234\ p_{\rm GeV}$. The probability of interaction for the mesons is negligible if the decay length is shorter than ~ 5 Km, that correponds to a column density $X = \ell\,\langle\rho\rangle$ of order of an interaction length ($\lambda_{\rm int} \simeq 120$ g cm^{-2}) for a non negligible fraction of the vertically produced mesons. This corresponds to $p \lesssim 100$, 180 and 750 GeV for $\pi^\pm$, K_L and $K^\pm$. One can conclude that for neutrinos with energy $E_\nu \lesssim 10$ GeV meson interactions are negligible, since essentially all parent mesons have unity decay probability. On the other hand, for $E_\nu \gtrsim 10$ GeV, it becomes essential to consider the competition between decay and interactions. Vertical mesons have smaller decay probability than horizontal ones because they are produced deeper in the atmosphere and travel into more dense layers of air (the air density decreases approximately exponentially with altitude). This effect is reflected in an enhancement of the ν horizontal fluxes over the vertical ones.

Only muon decay in air is of interest for neutrinos with energy $E_\nu > 50$ MeV. In fact the muons that reach the ground and penetrate into water or rock, rapidly stop and decay at rest, producing ν only with energy below $m_\mu/2$, that are not observed by the existing detectors. The probability that a $\mu^\pm$ decays in flight with momentum larger than $p_{\rm min}$, can be easily calculated as:

$$P_{\rm dec}(p_0, p_{\rm min}) = 1 - \exp\left[-\frac{m_\mu}{c\,\tau_\mu}\int_0^{x(p_{\rm min})} dx'\ \frac{1}{p(x')}\right] \tag{12}$$

where $p(x)$ and $x(p)$ are the momentum–depth relation and its inverse. The probability to decay with a momentum larger than few MeV's is only of order 10^{-3}. Calculations that claim a significant contribution from neutrinos produced below the surface must therefore must contain serious errors.

The difference between π^+ and π^- production constitutes perhaps the main source of uncertainty in the prediction of the standard–model μ/e ratio. The decay of π^+ results in ν_e, while the decay of π^- generates $\overline{\nu}_e$; in both cases a pair $(\nu_\mu,\overline{\nu}_\mu)$ is also produced. Existing large mass ν detectors do not have a magnetic field, and do not observe the charge of the final state lepton, therefore the observed rates sum over the ν and $\overline{\nu}$ contribution, that have different interaction cross section (with $\sigma_\nu > \sigma_{\overline{\nu}}$). Neglecting oscillations and in a very schematic notation that should be self–explaining, the rates for e–like and μ–like events are:

$$\begin{aligned} e &\propto \pi^+\sigma_\nu + \pi^- \ \sigma_{\overline{\nu}} \\ \mu &\propto \pi^+(\sigma_\nu + \sigma_{\overline{\nu}}) + \pi^- \ (\sigma_\nu + \sigma_{\overline{\nu}}) \end{aligned}$$

were we have used the fact that the three contributions $\pi^+ \to \nu_\mu$, $\pi^+ \to \overline{\nu}_\mu$, and $\pi^+ \to \nu_e$ are approximately equal. A larger π^+/π^- ratio leaves unchanged the fluxes of ν_μ and $\overline{\nu}_\mu$, but gives a larger $\nu_e/\overline{\nu}_e$ ratio. Because of the larger cross section ($\sigma_{\nu_e} > \sigma_{\overline{\nu}_e}$), this results in a larger rate of e–like events. Quantitatively:

$$\delta\left(\frac{\mu}{e}\right) \simeq -0.25\ \delta\left(\frac{\pi^+}{\pi^-}\right) \tag{13}$$

3.1. The role of Kaons

The contribution of kaons to the neutrino fluxes has two main sources, the most important one (analogous to the $\pi^\pm$ decay contribution) is due to the decay channel $K^+ \to \mu^+ + \nu_\mu$ (BR 63.5%) followed by the decay of the muon. In the first decay (differently from the pion case) the neutrino and the muon carry approximately equal energy: $\langle E_\mu\rangle/E_K = (1 + m_\mu^2/m_K^2) \simeq 0.522$, therefore the second generation ν's produced in muon decay carry on average only a fraction $\sim \frac{1}{2}\frac{1}{3} \simeq \frac{1}{6}$ of the kaon energy, significantly smaller than the energy fraction of the ν_μ directly produced in the $K^\pm$ decay. Since ν_e are produced in muon decay, the μ/e ratio for the ν's obtained from this source is therefore significanly larger that 2. On the other hand kaons can decay directly into ν_e via the channels $K^\pm \to \pi^0 + e^\pm + \nu_e(\overline{\nu}_e)$ (BR 4.8%) and $K_L \to \pi^\pm + e^\mp + \nu_e$ (BR 38.8%). There are of course also analogous channels into $(\mu^+\nu_\mu)$ or $(\mu^-\overline{\nu}_\mu)$ that have a little smaller branching ratios because of phase space suppression. The contribution of these channels to the ν flux has a μ/e ratio smaller than unity. Combining all kaon contributions to the ν fluxes, the resulting (no–oscillation) μ/e ratio remains similar to the naive value of 2 (approximately 15% higher). Uncertainties on the properties of kaon production, including the K/π ratio, K^+/K^- and $K_L/K^\pm$ are reflected in an estimated uncertainty of order $\delta(\mu/e) \sim 0.02$–0.03.

3.2. No oscillation up/down asymmetry

The neutrino yield for low energy primary particles is important for the estimate of the no–oscillation up–down asymmetry. This asymmetry arises because of the different geomagnetic cutoffs corresponding to different positions on the Earth. Down going neutrinos with zenith angle $\theta_{\rm down} < 90°$ and azimuth angle φ_ν are generated by primary particles reaching the Earth atmosphere in the vicinity of the detector and approximately the same direction ($\theta_0 \simeq \theta_{\rm down}$, $\varphi_0 \simeq \varphi_\nu$). These primary particles

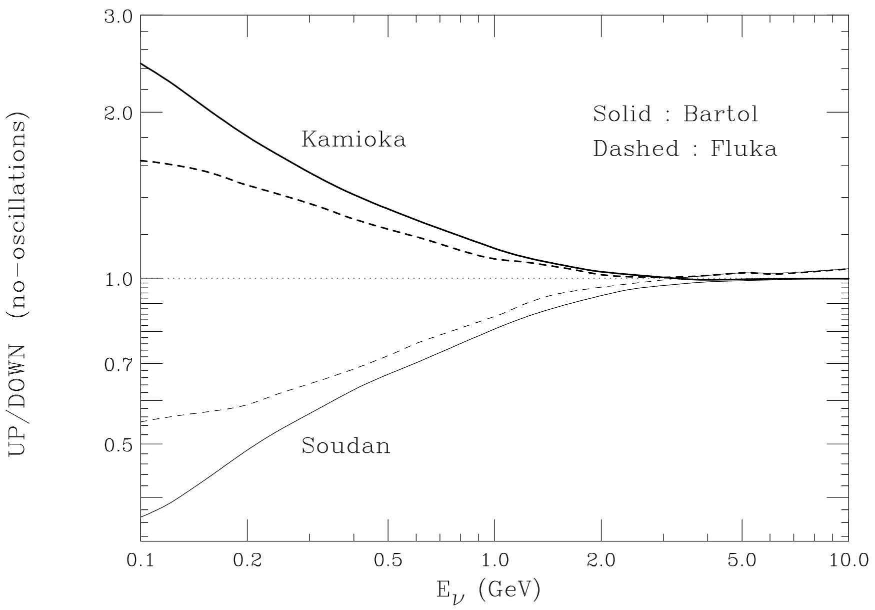

Fig. 11. Predictions for the no–oscillation up/down ratio for neutrinos (no smearing) with the Bartol and Fluka models.

have a cutoff $E_{\rm down}^{\rm min}$. Up–going neutrinos with zenith angle $\theta_{\rm up} \simeq 180 - \theta_{\rm down}$ (and the same azimuth angle) are generated by primaries that interact (with the same θ_0 and φ_0 of the down–going case) in a well defined region of the Earth that depend on the ν direction. These primary particles will have a different cutoff $E_{\rm up}^{\rm min}$. The difference between the up–going and down–going flux is therefore given by:

$$\phi_{\rm up} - \phi_{\rm down} = \int_{E_{\rm up}^{\rm min}}^{E_{\rm down}^{\rm min}} dE_0 \; \phi_0(E_0) \; Y_{p\to\nu}(E_0, \theta_0) \tag{14}$$

It can be seen that the up–down asymmetry depends on a correct description of the geomagnetic effects, and of the yield for low energy primaries.

The no–oscillation up/down ratio is larger than unity for the Kamioka site, reflecting the fact that the position of the detector corresponds to a magnetic latitude $\lambda_{\rm mag} \sim 27°$ close to the equator and therefore high geomagnetic cutoff for down–going neutrinos, while it is smaller than unity for the Soudan site (geomagnetic latitude $\lambda_{\rm mag} \simeq 55°$). The importance of the modeling of hadronic interactions for the up/down ratio is illustrated in fig. 11, that shows a plot of the up/down ratio calculated in the absence of oscillations for the SK and Soudan sites, using the same primary flux, and the FLUKA and Bartol interaction models. The ratio is approximately unity for $E_\nu \gtrsim 2$ GeV, independently from the interaction model, the up–down symmetry it is broken by geomagnetic effects at lower energy. The Bartol calculation, because of its larger ν–yield for low energy primaries has a large no–oscillation intrinsic asymmetry.

The model dependence of the non–oscillation asymmetry is especially important for the interpretation of the Soudan data, where the geomagnetic effects are larger, and because of smaller statistics only lower energy events can be used. The μ–like events of Soudan shows an excess of down–going events, that can be explained as the result of both oscillations and geomagnetic effects. The two effects (differently than for SK) have the same sign. In order to extract the oscillation–induced asymmetry, the geomagnetic one must be correctly subtracted.

In the near future we can expect some progres, thanks to the new HARP[36] experiment currently taking data at CERN. The physics motivations of the detector are a detailed study of $\pi^{\pm}$ production for the development of the first stage of a ν–factory, and at the same time a study of hadronic interactions for the calculation of the atmospheric ν fluxes.

4. Method of calculation: 3D versus 1D

The calculations of the atmospheric ν fluxes used to analyze the existing data have been performed in the so called "one–dimensional" approximation. All secondary particles produced in a shower are considered as exactly collinear with the primary particle. This is accomplished rotating all particles produced in each interaction (decay) so that they are collinear with the projectile (parent) particle, and neglecting multiple scattering and bending in the geomagnetic field. In this approximation one can study only the very small subset of primary particles, with trajectories that intersect the detector of interest, with an enormous reduction of the computational difficulty of the problem.

An important development has been the realization that this approximation introduces an important distortion of the angular distribution of low energy neutrinos that have a large average angle $\langle\theta_{0\nu}\rangle$ with respect to the primary particle direction. A 3–dimensional calculation, that takes into account the angle $\theta_{0\nu}$, predict an enhancement of the ν flux on the horizontal plane, that is more important with increasing $\langle\theta_{0\nu}\rangle$ (that is for decreasing E_ν). This enhancement can be understood as a simple geometrical effect [12,14]. The neutrinos received with zenith angle between θ and $\theta + d\theta$, are produced in a well defined "patch" of atmosphere, of area $dA = \ell^2(\theta)\ d\theta/\cos\theta_e$ where ℓ is the distance of the patch from the detector, and θ_e is the zenith angle of emission of the neutrino. The factor $1/\cos\theta_e$ takes into account the orientation of the patch of atmosphere with respect to line of sight, and is responsible for the enhancement near the horizontal plane (the factor ℓ^2 is canceled by a factor ℓ^{-2} due to the dispersion of the emitted neutrinos), since a source region of larger area absorbs more primary particles and emits more neutrinos. As an analogy, an observer inside (but not at the center) of a sperical shell of (isotropically emitting) stars sees an angular distribution of light $\propto \cos\theta_e^{-2}$, with an enhancement on the "horizontal" plane. This effect vanishes when the ν's are emitted nearly collinearly with the primary particle, since in this case one has to consider only the primary particles that arrive with the same ν direction, and the effective area of the atmosphere patch is then

$dA_{\rm proj} = dA \cos\theta_e$, exactly canceling the source area effect. The up–down symmetry of the (no–oscillation) fluxes remain rigorously valid also in a 3-D treatment.

The enhancement on the horizontal plane for low energy neutrinos, is difficult to observe directly because of the poor experimental angular resolution of the existing detectors. However since it implies a different pathlength distribution for the neutrinos, it can in principle have non–trivial consequences for the interpretation, for example on the Δm^2 allowed regions. Preliminary analysis of the SK data suggest that the effect on the allowed region is only a modest shift.

5. The muon flux constraints

The fluxes of atmospheric muons are strictly related to the neutrino ones, because almost all ν's are produced either in association with, or in the decay of $\mu^\pm$. Precise measurements of the muons offer then a way to check directly the ν fluxes. To constraint the flux of neutrinos with energy E_ν, the most interesting muons are those created with energy around $E_\mu \sim 2\ E_\nu$ (the factor of two being a kinematical effect). The most important range of ν energy is $E_\nu \sim 0.1$–10 GeV, and especially for the lowest part of this range, only a vanishing or small fraction of the related muons reach the ground because of energy loss (the atmosphere corresponds to a loss of ~ 2 GeV for a vertical muon) and decay (the μ decay length is $\ell_\mu \simeq 6.2\ p_\mu({\rm GeV})$ km). For low energy muons the measurement is possible only at high altitude.

The authors of the existing atmospheric ν calculations checked that their predictions for the muon flux (that is 'automatically' calculated together with the ν flux) with the existing muon data[27,28)] at ground level. To a large extent the agreement between the HKKM and Bartol calculations of the ν fluxes, that is the effect of a cancellation between different estimates of the primary flux and different modelings of the hadronic interaction, is not casual, but the result of the μ constraint. Recently new measurements[29,30,17)] of the ground level muon flux, have been performed with detectors developed for balloon flights. The new data suggests that previous estimates could be too high.

6. Calculations of the atmospheric ν fluxes

The first calculations of the atmospheric neutrino fluxes were performed integrating numerically a set of differential equations that describe the evolution of the different components of hadronic showers[7,8,9)]. More accurate calculations are based on Montecarlo methods like those by the Bartol group[10)] and by Honda, Kajita, Kasahara and Midorikawa (HKKM)[11)] that have been used extensively for comparison with the experimental data.

More recently the FLUKA group[12)] has performed a calculation of the atmospheric ν–fluxes based on the FLUKA code, that for the first time has abandoned the so called "one dimensional" approximation, in which all secondaries (including the neutrinos) produced in a c.r. showers are exactly collinear with the primary particles. The group has made available tables of ν fluxes for different locations at the web site[13]. A technical limitation of the FLUKA calculation is the approximation to neglect the effects of the magnetic field during the development of a shower. This approximation, because of the assumed spherical symmetry, allows to "use" many times the same MC shower, transporting it (with translations and rotations) to different points of the Earth, with an enormous saving in computation time.

The effects of the bending of secondary particles in the geomagnetic field has been studied in[14], where it was found to be observable, and in fact perhaps already observed, in the east–west asymmetries of μ–like and e–like events[25]. A 3–dimensional calculation of the neutrino fluxes has also been performed by the group of Tserkovnyak et al[15],

The differences between the results of the calculations of the three Bartol[10], HKKM[11] and FLUKA[13] have been studied in detail. These differences are about the absolute normalization, and the shapes of the energy spectra and zenith angle distributions of the ν fluxes. The origin of these differences can be reasonably well traced back to (a) differences in the choice of the input c.r. primary spectrum, (b) differences in the description of particle production in hadronic interactions, (c) inclusion or not of the approximation of "collinearity" of the secondary particles in the shower (or 3D versus 1D in the jargon of the field). This understanding implies the modeling of the showers (that is the description of energy losses, kinematics of particle decays, muon polarization effects and so on) is essentially equivalent in the three independent codes, giving confidence of their correctness.

After this conference a new calculation of the neutrino fluxes of V. Plyaskin[39] has been made public. This calculation differs significantly from previous results. The differences are: (a) a much softer neutrino energy spectrum, (b) a much stronger no–oscillation up/down asymmetry, (c) a stronger enhancement of the horizontal plane. The reasons for these differences are not at present understood. Some remarks however are in order. The first remark is that primary p flux used in[39] is very similar to the flux used in other calculations for all zenith angles. The author of[39] does not use the Liouville theorem result (equation (8) and starts from an isotropic cosmic ray flux at a distance of 10 Earth radii (with an efficiency of only 10^{-4}). However for a static magnetic field (and avoiding numerical errors) the approaches are identical. In fact it has been verified that the input primary spectra for the Plyaskin and Bartol calculations are very similar for all angles. In the Plyaskin calculation one takes also into account the incident fluxes of subcutoff particles, however they give only a neglible contribution to the ν fluxes (see the discussion in sec.2.3). In conclusion the difference has its origin in a different treatment of the development of the hadronic showers. The potentially most interesting result of Plyaskin is a large no–oscillation asymmetry. Note that for the SK site this large asymmetry is approximately of the same size for

e–like and μ–like events and is an *excess* of up–going events, in agreement with the sign of previous authors but in strong disagreement with the data that exhibits a U/D ratio much smaller than unity for μ–like events and approximately unity for e–like events. Therefore if the results of Plyaskine are correct they would also require new physics, and in fact of more complicated form. A third remark is that the spectrum predicted in[39] appears to be much softer that the data. The tentative conclusion is that the calculation[39] contains technical mistakes. A hint of this is coming from the claim to have obtained a significant contribution to the ν fluxes from neutrinos created below the Earth's surface. This claim is obviously incorrect, since essentially all muons that reach the ground (or the ocean) stop before decaying at rest and can only produce neutrinos with $E_\nu \le m_\mu/2 \simeq 50$ MeV, below the detection threshold.

7. Interpretation of the data

A complete discussion of effects of the uncertainties in the prediction of the atmospheric ν fluxes on the interpretation of the data is beyond the scope of this work. Here we will only make some brief comments about the simplest (and most natural) interpretation in terms of two–flavor $\nu_\mu \leftrightarrow \nu_\tau$ oscillations. In this case the survival probability for ν_μ and $\overline{\nu}_\mu$ has the form:

$$P_{\nu_\mu \to \nu_\mu} = 1 - \sin^2 2\theta \ \sin^2 \left[\frac{\Delta m^2 L}{4\, E_\nu} \right], \tag{15}$$

that depends on the ratio L/E_ν and the two parameters $\sin^2 2\theta$ and Δm^2. The expression (15) takes simple forms when the ratio L/E_ν is much larger or much smaller than $|\Delta m^2|^{-1}$. For small L/E_ν the probability is approximately unity, while for large L/E_ν, averaging over the fast oscillations, one has: $\langle P_{\nu_\mu \to \nu_\mu} \rangle \sim 1 - \sin^2 2\theta/2$. Note that these 'asymptotic' forms are independent from Δm^2.

As illustrated in fig. 12 the ν pathlength L is strongly correlated with the ν zenith angle θ_z (the correlation is not perfect because the ν creation point is not known). Note that the pathlength L spans three order of magnitude, with more than one decade of L corresponding to a narrow range of angles close to the horizontal. For example when θ_z is between ± 10 degrees from the horizontal, L varies in the interval 150–2400 Km.

Because of the good correlations between L and $\cos\theta_z$ it is possible to consider the oscillation probability as a function of $\cos\theta_z$ and E_ν. As an example in fig. 13 are shown curves of constant survival probability in the plane $(E_\nu, \cos\theta_z)$ assuming maximal mixing and $\Delta m^2 = 3 \times 10^{-3}$ eV^2. Some qualitative remarks are the following:

1. For $E_\nu \lesssim 5$ GeV (that corresponds to the sub and multi–GeV region), or essentially the entire up–going hemisphere ($\cos\theta_z < 0$) the oscillation probability oscillates rapidly, and can be reasonably well approximated with the average value $\langle P_{\nu_\mu \to \nu_\mu} \rangle \simeq 1 - \sin^2 2\theta/2 = 1/2$.

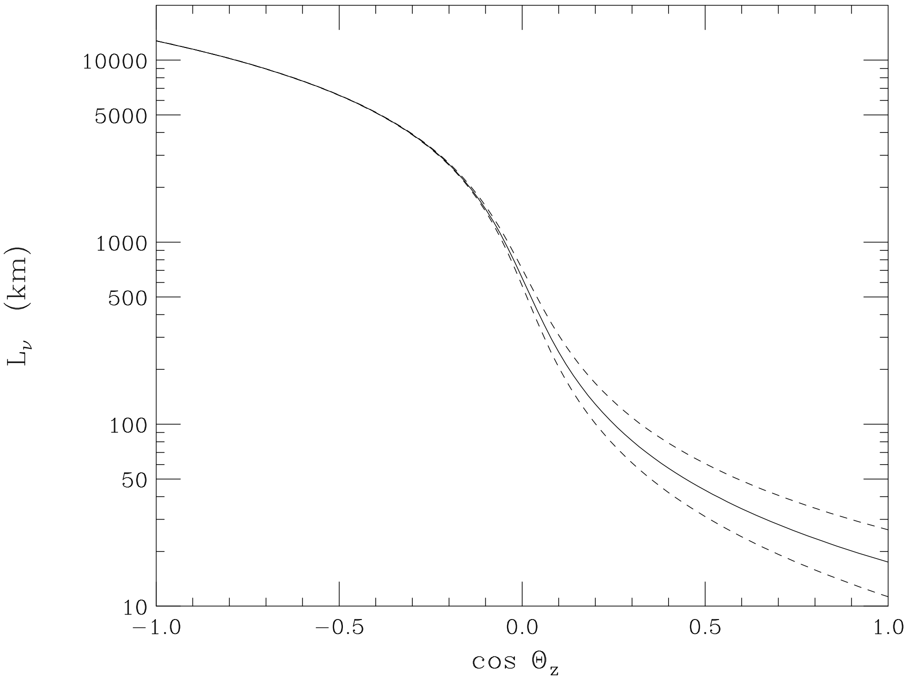

Fig. 12. The solid line shows the most probable L for ν produced directly in π and K decay, plotted as a function of the ν zenith angle. The dashed lines show the width of the distribution that contains 68% of the ν creation points.

2. In a large fraction of the down–going hemisphere ($\cos\theta_z > 0$), the survival probability is approximately unity, while neutrinos near the horizontal are still significantly suppressed.

3. For high energy $E_\nu \simeq 10$–100 GeV the oscillation probability differ significantly from unity only for very long pathlength neutrinos, with the horizontal flux essentially unchanged.

These qualitative features match beautifully the experimental effects detected by SK[1)]. For multi–GeV events, when the correlation between muon and neutrino is good, the down–going events are essentially unchanged, while up–going events are suppressed by the average factor $\langle P_{\nu_\mu \to \nu_\mu}\rangle$ and horizontal ones have an intermediate suppression. For sub–GeV events the angle averaged suppression is similar to the multi–GeV case, but the detected distortion of the zenith angle distribution is less strong, because of the poor correlation between lepton and neutrino. Finally up–going muons, with a median energy of order ~ 100 GeV, have a suppression smaller than for multi–GeV but still sizable. In this case only up–going neutrinos are detected, and therefore an up–down comparison is not possible, however one expects a distortion of the zenith angle distribution of the up–going events, since only the quasi–vertical ones are suppressed.

The determination of $\sin^2 2\theta$ benefits from the fact that for $E_\nu \simeq 1$ GeV, the region of L that corresponds to the "transition region" corresponds in zenith angle to the horizontal plane. In this situation, it is a reasonable approximation to use the "asymptotic forms" for large and small L/E_ν for the oscillation probability in the vertically up–going and down–going regions, and one extract the value of $\sin^2 2\theta$ with a very weak dependence on the estimate of Δm^2. The method is based on the robust prediction of approximately up–down symmetric fluxes in the absence of oscillations. Using the notation U, D, U_0 and D_0 for the observed and predicted rates of up–going and down–going μ–like contained events, one expects $D \simeq D_0$, $U \simeq U_0(1 - \sin^2 2\theta/2)$ with $D_0 \simeq U_0$. The mixing parameter can then be obtained inverting the relation:

$$\frac{U}{D} \simeq 1 - \frac{1}{2}\ \sin^2 2\theta \tag{16}$$

The two most important corrections (and possible sources of systematic error) to obtain the mixing parameter from this measurement are the existence of a no–oscillation asymmetry (present even in the absence of new physics), and the effects of the finite resolution of the detector. The no–oscillation asymmetry arises because of geomagnetic effects, with additional contributions due to the presence of mountains above the detector sites, and possibly because of a latitude dependence of the atmospheric profile. These effects can be calculated and corrected for. A comparison between e–like and μ–like events provide a check on the correction. For the SK multi–GeV events $U_0/D_0 - 1$ is estimated to be ~ 0.02 with a sign that is unambiguosly predicted to be opposite to the oscillation effect.

The finite resolution in the reconstruction of the ν direction results in a measured asymmetry (for the reconstructed direction) smaller than the true ν asymmetry. The angular resolution is dominated by the size of the angle $\theta_{\mu\nu}$ between the detected muon and the neutrino, that shrinks approximately $\propto E_\mu$. As a consequence the ν asymmetry is essentially unobservable for $E_\mu < 0.4$ GeV, and results in a much smaller μ asymmetry for sub–GeV events. The correction is also non negligible for multi–GeV events, where maximal mixing corresponds to an up/down ratio of order 0.55, and not 0.50 as one could naively expect. Increasing E_μ the correction due to the resolution is smaller, however the number of detected event is reduced, and the statistical error grows. Multi–GeV events are close to the "optimum choice" for the determination of the mixing parameter balancing statistics and resolution. Systematic uncertainties on the "finite resolution correction" exist because of uncertainties in the description of the ν cross section, (especially about nuclear effects that play a crucial role), and also because of uncertainties in the precise shape of the non–oscillation zenith angle distribution near the horizontal direction, since it the misreconstruction of quasi–horizontal events that dilute the true asymmetry. For a higher horizontal flux the correction due to the finite angular resolution becomes more important. At present however the allowed interval for $\sin^2 2\theta$ is still controlled by the statistical errors on the multi–GeV sample. With additional data, the allowed interval will shrink, and it

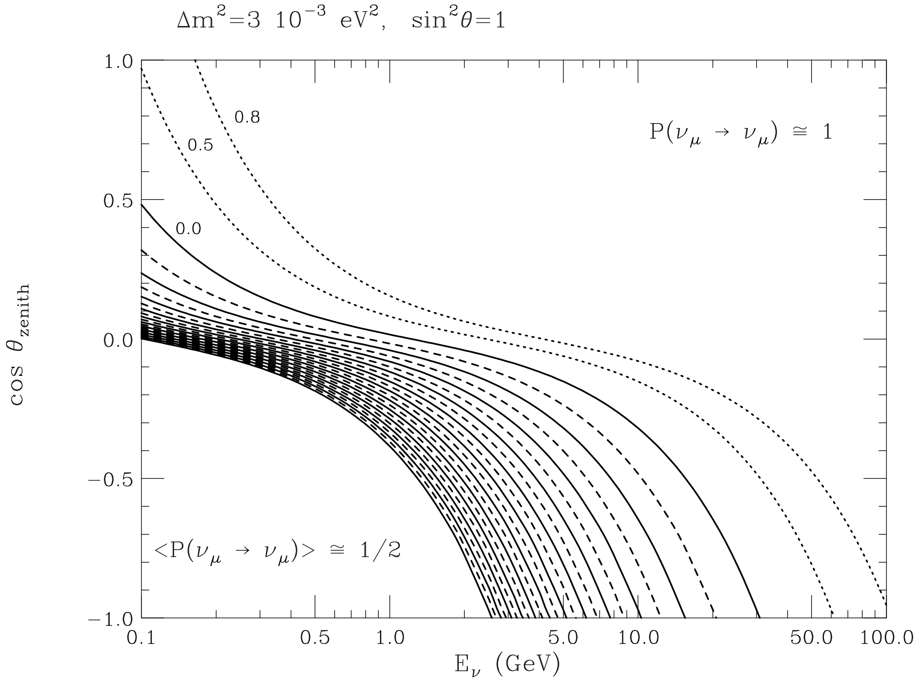

Fig. 13. Curves of constant survival probability in the plane $(E_\nu, \cos\theta_z)$. The solid curves give $P_{\nu_\mu\to\nu_\mu} = 0$, the dashed curves give $P_{\nu_\mu\to\nu_\mu} = 1$. The curves are not plotted in the region (low E_ν and $\cos\theta_z < 0$) where they are very dense. The curves are calculated for the choice of parameters $\Delta m^2 = 3 \times 10^{-3}$ eV^2 and $\sin^2 2\theta = 1$.

will it will become important to consider more carefully the systematic uncertainties in the prediction.

To estimate the value of Δm^2 one needs to study the oscillation probability in the "transition region" that corresponds to of $L/E_\nu \sim |\Delta m^2|^{-1}$. The survival probability has in fact its "first" minimum[c]when L/E_ν is equal to a "critical value":

$$\left(\frac{L}{E_\nu}\right)_{\rm crit} = \frac{2\pi}{|\Delta m^2|} \simeq 412 \left(\frac{3\times 10^{-3}~{\rm eV}^2}{|\Delta m^2|}\right) \frac{\rm Km}{\rm GeV} \tag{17}$$

For $E_\nu \simeq 1$ GeV and Δm^2 in the interesting range $|\Delta m^2| \sim 10^{-3}$–$10^{-2}$ eV^2 this corresponds to zenith angles close to the horizontal plane. This situation, is ideal to measure $\sin^2 2\theta$, since the quasi–vertical down–going (up–going) events correspond then to small (large) L/E_ν and therefore to the asymptotic forms of the oscillation probability. On the other hand, the estimate of Δm^2 is particularly difficult, because the resolution in L is very poor near the horizontal, reflecting the fact that when the zenith angle is close to $\theta_z \sim 0°$, the pathlength L varies very rapidly with θ_z, and a small error on the zenith angle is reflected in a large uncertainty on L. Moreover, it is of course impossible to use the comparison of the up-going and down–going fluxes to reduce systematic uncertainties. In this situation the experimental determination

[c]The first minimum, corresponds to the shortest L for a fixed E_ν, or the highest E_ν for a fixed L.

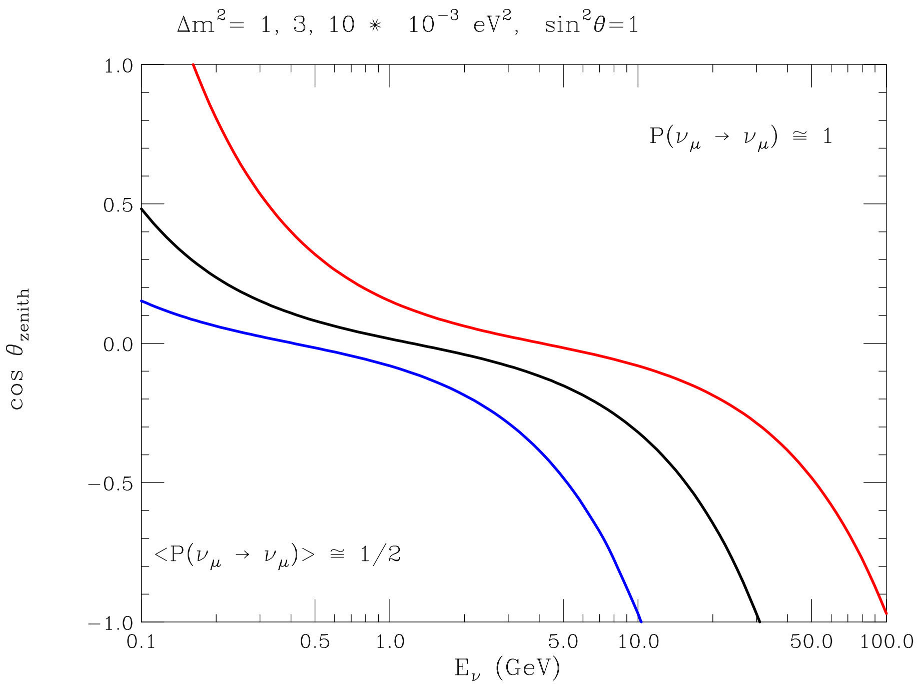

Fig. 14. Curves in the plane $(E_\nu, \cos\theta_z)$ that correspond to the first (highest energy) minimum of the survival probability. The three curves correspond to $\Delta m^2 = 1$, 3 and 10 in units of 10^{-3} eV^2.

of Δm^2 is controlled by the suppression of the μ–like event rate integrated over a broad angular range around the horizontal plane. To estimate this suppression, the two key theoretical inputs are the predictions of the zenith angle distribution of the ν fluxes, and of the μ/e ratio. The suppression of the μ–like event rate, for the range of Δm^2 indicated by the data, decreases with increasing Δm^2, since more ν's with shorter pathlengths can also oscillate. To estimate the effect quantitatively one needs obviously to know with precision the shape of the zenith angle distribution of the ν fluxes. The prediction for the μ/e ratio is essential as a constraint. Because of this, theoretical and systematic uncertainties are likely to be already the dominant source of error in the estimate of Δm^2.

The same reasons that are at the origin of the difficulties in the estimate of Δm^2 for an interpretation of the data, in terms of $\nu_\mu \leftrightarrow \nu_\tau$ oscillations, can explain the possibility to explain the data with a survival probability that decreases monotonically with increasing L/E_ν, instead of the oscillating form. Physical models that result in a probability $P_{\nu_\mu \to \nu_\mu}$ with this form have been constructed as a form of neutrino decay[37], or as decoherence[38].

8. Summary

In the last two years there has been some significant progress in the calculation of the atmospheric neutrino fluxes. New "second generation" calculations are under development and will soon become available. The main lessons of these critical investigations has been the confirmation that the evidence for new physics in the atmospheric ν data is robust. For the two–flavor oscillation scenario that is the simplest and probably most successful explanation of the data, no large theoretical bias in the parameter dermination has been found. The uncertainty of $\sin^2 2\theta$ is controled by the measuremenys of the up/down asymmetry of the SK multi–GeV μ–like events and is dominated by statistical errors. The determination of Δm^2 depends on the measurement of the μ/e ratio and the up/down asymmetry of sub–GeV events. In this case the theoretical (and experimental) systematic uncertainties are important, and control the extension of the allowed region.

9. Acknowledgements

I would like to thank Milla Baldo Ceolin for the invitation to this workshop, Giuseppe Battistoni, Alfredo Ferrari, Tom Gaisser, M.Honda, Takaaki Kajita, Maurizio Lusignoli, Todor Stanev and Silvia Vernetto for many useful discussions.

10. References

1) Super-Kamiokande coll.(Y. Fukuda *et al.*), Phys. Rev. Lett. **81**, 1562 (1998).
2) C. McGrew, these Proceedings.
3) Kamiokande Collaboration (K.S. Hirata *et al.*), Phys. Lett. **B 205**, 416 (1988); Phys. Lett. **B 280**, 146 (1992); (Y. Fukuda *et al.*), Phys. Lett. **B 335**, 237 (1994).
4) IMB Collaboration, (D. Casper *et al.*), Phys. Rev. Lett. **66**, 2561 (1991); IMB Collaboration, (R. Becker-Szendy *et al.*), Phys. Rev. **D 46**, 3720 (1992).
5) Soudan 2 Collaboration (W.W.M. Allison *et al.*), Phys. Lett. **B 449**, 137 (1999);
6) MACRO Collaboration (M. Ambrosio *et al.*), Phys. Lett. **B 434**, 451 (1998); F. Ronga (for the MACRO Collaboration), in Proceedings of Neutrino'98, Takayama, Japan, (1998), hep-ex/9810008.
7) L.V. Volkova, Yad.Fiz. 31, 1510 (1980), also in Sov.J.Nucl.Phys. **31**, 784 (1980).
8) A.V. Butkevich, L.G. Dedenko and I.M. Zheleznykh Yad.Fiz. **50**, 142, (1989) or Sov.J.Nucl.Phys. **50**, 90 (1989).
9) E. V. Bugaev and V. A. Naumov, Phys.Lett. **B 232** (1989) 391.
10) G. Barr, T.K. Gaisser and T. Stanev, Phys. Rev. **D 39**, 3532(1989); V. Agrawal, T.K. Gaisser,P. Lipari and T. Stanev, Phys. Rev. **D 53**, 1314 (1996). P. Lipari, T.K. Gaisser and T. Stanev, Phys. Rev. **D 58**, 073003 (1998).

11) M. Honda, T. Kajita, K. Kasahara & S. Midorikawa, Phys. Rev. **D 52** (1995) 4985.
12) G. Battistoni, A. Ferrari, P. Lipari, T. Montaruli, P. R. Sala and T. Rancati, Astropart. Phys. **12**, 315 (2000), [hep-ph/9907408].
13) www.mi.infn.it/˜battist/neutrino.html
14) Paolo Lipari, Astropart. Phys. **14**, 153 (2000), [hep-ph/0002282];
Astropart. Phys. **14**, 171 (2000), [hep-ph/0003013].
15) Y. Tserkovnyak, R. Komar, C. Nally and C. Waltham, hep-ph/9907450
16) The AMS Collaboration, Phys.Lett. **B 472**, 215 (1999).
17) Bess Collaboration (T. Sanuki *et al.*), Ap.J. **545**, 1135 (2000). [astro-ph/0002481]
18) W.R. Webber, R.L. Golden & S.A. Stephens, Proc. 20th ICRC (Moscow) vol. 1 (1987) 325.
19) G. Barbiellini, *et al.*, Proc. 25th ICRC (Durban) vol. 3 (1997) 369. Also, M. Boezio *et al.* INFN-AE-98-06.
20) M.J. Ryan, J.F. Ormes and V.K. Balasubrahmanyan, Phys. Rev. Lett. **28**, 985, (2000).
21) JACEE Collaboration (K. Asakimori *et al.*), Ap.J. **502**, 278 (1998).
22) The AMS Collaboration, Phys.Lett. **B 484**, 10 (2000).
23) The AMS Collaboration, Phys.Lett. to appear (2001).
24) Paolo Lipari, Astrop.Phys. to appear (2001). [astro-ph/0101559]
25) Super–Kamiokande Collab. (Futagami *et al.*), Phys. Rev. Lett. **82**, 5194 (1999). [hep-ex/9901139].
26) G. Lemaître and M.S. Vallarta, Phys. Rev. **43**, 87, (1933).
27) O.C. Allkofer, O.C. Karstensen and W. D. Dau, Phys. Lett. **B 425** (1971).
28) B.C. Rastin, J. Phys. **G 10**, 1629 (1984).
29) M.P. De Pascale *et al.*, J. Geophys. Res. **98**, 3501 (1993).
30) J. Kremer *et al.*, Phys. Rev. Lett. **83**, 4241 (1999).
31) Engelmann et al. (HEAO–3 Collaboration), Astr. Astr. **148**, 12 (1985).
32) D. Muller et al (CRN Collaboration), Ap. J **374**, 356 (1991).
33) G. Fiorentini, V.A. Naumov and F.L. Villante, hep-ph/0103322.
34) H. Lee and Y. S. Koh, Nuovo Cimento **B 105**, 883 (1990).
35) P. Lipari, M. Lusignoli and F. Sartogo, Phys. Rev. Lett. **74**, 4384 (1995).
36) `http://harp.web.cern.ch/harp/`
37) V. Barger, J.G. Learned, P. Lipari, M. Lusignoli, S. Pakvasa, & T.J. Weiler, Phys.Lett. **B 462**, 109 (1999). [hep-ph/9907421]
38) E. Lisi, A. Marrone and D. Montanino, Phys. Rev. Lett. **85**, 1166 (2000).
39) V. Plyaskin, hep-ph/0103286